

Article

Morpho-Constitutional Classification of Urinary Stones as Prospective Approach for the Management of Human Pathological Biomineralization: New Insights from Southern Italy

Francesco Izzo ¹, Alessio Langella ¹, Chiara Germinario ², Celestino Grifa ², Ettore Varricchio ², Maria Chiara Di Meo ², Luigi Salzano ³, Giuseppe Lotrecchiano ³ and Mariano Mercurio ^{2,*}

¹ Department of Earth Sciences, Environment and Resources, University of Naples Federico II, Via Cintia, 80126 Naples, Italy

² Department of Science and Technology, University of Sannio, Via de Sanctis snc, 82100 Benevento, Italy

³ UOC Urology, San Pio Hospital, Via dell' Angelo, 82100 Benevento, Italy

* Correspondence: mariano.mercurio@unisannio.it



Citation: Izzo, F.; Langella, A.; Germinario, C.; Grifa, C.; Varricchio, E.; Di Meo, M.C.; Salzano, L.; Lotrecchiano, G.; Mercurio, M. Morpho-Constitutional Classification of Urinary Stones as Prospective Approach for the Management of Human Pathological Biomineralization: New Insights from Southern Italy. *Minerals* **2022**, *12*, 1421. <https://doi.org/10.3390/min12111421>

Academic Editor: Yannicke Dauphin

Received: 13 October 2022

Accepted: 7 November 2022

Published: 9 November 2022

Publisher's Note: MDPI stays neutral with regard to jurisdictional claims in published maps and institutional affiliations.



Copyright: © 2022 by the authors. Licensee MDPI, Basel, Switzerland. This article is an open access article distributed under the terms and conditions of the Creative Commons Attribution (CC BY) license (<https://creativecommons.org/licenses/by/4.0/>).

Abstract: The present investigation exposes the main results raised from an active collaboration started in 2018 with the San Pio Hospital (Benevento, Southern Italy), aiming at a detailed mineralogical investigation of urinary stones of patients from the Campania region. Forty-nine uroliths (both bladder and kidney stones) have been surgically collected from patients admitted between 2018 and 2020 at the Department of Urology of the San Pio Hospital and characterized for clinical purposes and environmental biomonitoring from a mineralogical point of view. Possible causes and environmental implications were inferred according to the morpho-constitutional classification of the uroliths carried out by means of a conventional analytical approach. The mineralogical frequency distribution of uroliths from the Campanian region can be discussed as a function of dietary, socio-demographic, and environmental risk factors. Whewellite [$\text{CaC}_2\text{O}_4 \cdot \text{H}_2\text{O}$] and weddellite [$\text{CaC}_2\text{O}_4 \cdot (2+x)\text{H}_2\text{O}$], along with anhydrous calcium oxalate, represent the main mineralogical phases forming the biominerals examined here. Worth to note is that the percentage of oxalates in the Campanian region (ca. 51%) is quite comparable to those of other Mediterranean areas. Frequent uricite [$\text{C}_5\text{H}_4\text{N}_4\text{O}_3$] (ca. 33%), mainly observed in bladder stones of older male patients, could be related to an incorrect lifestyle and dietary habits. Occurrence of lower percentages of phosphate (i.e., brushite [$\text{CaHPO}_4 \cdot 2(\text{H}_2\text{O})$] and carbonated apatite [$\text{Ca}_{10}(\text{PO}_4\text{CO}_3)_6(\text{OH})_8$] and mixed stones (such as, for example, a mixture of ammonium urate [$\text{NH}_4\text{C}_5\text{H}_3\text{N}_4\text{O}_3$] and calcium oxalates) indicates specific etiopathogenetic mechanisms, suggesting proper therapeutical approaches.

Keywords: biomineral; urinary stone; microscopy; spectroscopy; calcium oxalate; carbonated apatite; brushite; ammonium urate; uricite; human health

1. Introduction

One of the leading questions from which this research arises is: why mineralogists who apply their knowledge to improve human well-being should study biominerals such as human urinary stones? Is there anything they can provide as a further scientific contribution to fuel the debate on this issue? Probably, the only scientific curiosity driving the activity of a scientist may not be enough to intercept the real challenge. For this reason, we considered it mandatory to directly involve urologists in this process, which could give us some relevant information on account of their continuous interaction with patients suffering from this pathology, which defines manifest economic burdens to the national health system. The first important issue emerging from this collaboration was the almost total lack of information on how the disease spreads on a regional scale and, above all,

whether it is still possible to find the right prevention so that the discomfort caused by the effects can be minimized. However, the causes that trigger the illness at a certain point in the patient's life still represent the real knot to untie. From these premises derives the multidisciplinary approach that has been thought to give to the characterization of human urinary stones also on account of the significant number of people suffering from this pathology [1–4]. On the other hand, the many steps forward that have been made from a pharmacological and surgical point of view were not sufficiently counterbalanced by efforts to solve the problem without recurring invasive interventions. To overcome this drawback, a convergence of energy and knowledge is strongly required, using a multidisciplinary approach, which cannot disregard a preliminary and in-depth knowledge of the stone mineralogy. Current literature reports much research on the mineralogical characterization of urinary stones, with a specific emphasis on the morpho-constitutional aspects required for correct classification and the most appropriate analytical methods necessary for a proper characterization of these biominerals [5–10]. However, despite the great number of research dealing with the morphological and compositional classification of human uroliths all around the world, very little has been done for Italian contexts [11,12].

Nucleation of pathological calcifications can arise from different mechanisms recently overviewed by Bazin et al. [13,14]. Generally, nephrolithiasis can be considered the result of crystal formation, aggregation, and retention in the kidney, related to homogeneous and heterogeneous nucleation mechanisms [13]. Another interesting study was published by Sivaguru et al. [15], which sheds new light on the mechanisms that control the shift between biotic and abiotic processes during biomineralization.

Following these schemes, new scenarios can be offered to the scientific community that consider the set of information that the stone contains, comparable to a tape that records all the variations induced by the environment in which the human being lives (including eating habits, lifestyle, working activity, breathed air, etc.).

From these bases, several studies emerged focusing on trace elements and their role as possible geomarkers of geographical traceability [16–20]. The same attention, currently disregarded, should be placed to the investigation of the types of biomineralizations that develops in specific contexts, such as the Italian one.

In the recent past, Giannossi et al. [12], studying kidney stones from the Basilicata region (Southern Italy), evidenced how the mineralogical approach, aimed at improving the morphological investigation, helped to associate some pathological conditions, such as a geographical differentiation, to the specific mineralogical characteristic of the observed stones. In other words, this study could be configured as one of the first ever aimed at a spatial mapping of the spread of urolithiasis on a territory, which associates a specific eating behavior (with specific attention to the quality of the local spring waters) to an analogous characteristic biomineralization.

Mercurio et al. [11] showed how an in-depth and multidisciplinary study on bladder stones from the Campania region (Southern Italy) can give very useful information to be used as starting point for further investigations addressed to the identification of this link between the territory and urolithiasis.

The present paper is an in-depth mineralogical characterization of a significant number of urinary stones from patients admitted to the Department of Urology of the San Pio Hospital in Benevento. The research cluster here proposed still aims at finding reliable and preliminary interpretations for the urolithiasis that afflicts patients in the Campania region and in particular those who live in inland areas.

2. Materials and Methods

Urinary stone samples have been surgically collected from 49 patients (7 females and 42 males) admitted to the Department of Urology of the San Pio Hospital (Benevento, Italy) between the 2018 and the 2020. The set of biominerals here examined also includes for comparison six bladder stones (KS006B, KS011B, KS012B, KS020B, KS022B, KS023B)

already characterized in a previous investigation [11] and here further analyzed by scanning electron microscopy [21].

The samples were labeled using the code abbreviation KS (namely kidney stones) and a three-digit sequential number followed by a letter B for bladder stones. Before stone analyses, all samples were extensively washed by distilled water in order to remove impurities due to the occurrence of residual amorphous organic matter not belonging to the biomineral aggregate. In some cases, traces of this organic matter could be detected by FTIR analyses or by microscope observations.

Clinical interviews were also held, in anonymous form, to gather some useful information about patient's medical history and lifestyle (Table 1). Apart from the patient KS010 coming from Vibo Valentia (Calabria, Italy), all the patients (24–83 years old) reside in Campania region with the following distribution: 30 from Benevento, 7 from Avellino, 5 from Caserta, 5 from Naples, and 1 from Salerno. Comorbidities were also declared during clinical interviews and reported in Table 1.

Table 1. Patient's personal details. M, male; F female; Age expressed in years; BMI, body mass index; * from [11].

n.	ID Sample	Sex	Age	Occupation	Body Weight	Height	BMI	Calculus Weight	Other Diseases §
1	KS001	M	28	Farmer	62 kg	169 cm	21.7 kg/cm ²	29 mg	-
2	KS002	M	54	Architect	95 kg	175 cm	31.0 kg/cm ²	15 mg	DLP
3	KS003	M	63	Farmer	78 kg	172 cm	26.4 kg/cm ²	47 mg	DM
4	KS004	F	69	Housewife	65 kg	165 cm	23.9 kg/cm ²	50 mg	HTN, OP
5	KS005	M	35	Farmer	70 kg	175 cm	22.9 kg/cm ²	13 mg	-
6	KS006B *	M	76	Retired	78 kg	175 cm	25.5 kg/cm ²	1086 mg	-
7	KS007	F	60	Housewife	74 kg	160 cm	28.9 kg/cm ²	280 mg	DM, UC
8	KS008	M	53	Cook	85 kg	175 cm	27.8 kg/cm ²	325 mg	HTN
9	KS009	M	51	Farmer	87 kg	185 cm	25.4 kg/cm ²	101 mg	-
10	KS010	M	39	Driver	70 kg	170 cm	24.2 kg/cm ²	10 mg	-
11	KS011B *	M	75	Farmer	69 kg	165 cm	25.3 kg/cm ²	531 mg	DM, HTN
12	KS012B *	M	73	Farmer	90 kg	175 cm	29.4 kg/cm ²	1553 mg	ASHD
13	KS013	M	42	Researcher	74 kg	180 cm	22.8 kg/cm ²	20 mg	-
14	KS014	M	74	Retired	50 kg	170 cm	17.3 kg/cm ²	20 mg	-
15	KS015	M	54	Office worker	78 kg	175 cm	25.5 kg/cm ²	41 mg	-
16	KS016	M	57	Railway man	85 kg	178 cm	26.8 kg/cm ²	51 mg	HTN
17	KS017	M	57	Merchant	70 kg	180 cm	21.6 kg/cm ²	9 mg	GERD
18	KS018	M	54	Physician	82 kg	175 cm	26.8 kg/cm ²	24 mg	GERD
19	KS020B *	M	67	Barman	78 kg	165 cm	28.7 kg/cm ²	1050 mg	DLP
20	KS021	M	64	Accountant	84 kg	180 cm	25.9 kg/cm ²	98 mg	ASHD
21	KS022B *	M	76	Farmer	74 kg	170 cm	25.6 kg/cm ²	3150 mg	-
22	KS023B *	M	75	Office worker	75 kg	165 cm	27.5 kg/cm ²	9750 mg	HTN
23	KS024	F	40	Housewife	101 kg	160 cm	39.5 kg/cm ²	18 mg	HTN, DTR
24	KS025	F	36	Housewife	98 kg	160 cm	38.3 kg/cm ²	16 mg	DTR, RF
25	KS026	M	52	Office worker	81 kg	178 cm	25.6 kg/cm ²	70 mg	-
26	KS027	M	63	Office worker	85 kg	174 cm	28.1 kg/cm ²	100 mg	-
27	KS028B	M	67	Physician	82 kg	176 cm	26.5 kg/cm ²	530 mg	ASHD
28	KS029B	M	78	Office worker	74 kg	180 cm	22.8 kg/cm ²	3700 mg	DM
29	KS030	M	59	Physician	86 kg	178 cm	27.1 kg/cm ²	180 mg	ASHD
30	KS031	F	24	Workman	48 kg	160 cm	18.8 kg/cm ²	30 mg	-
31	KS032B	M	68	Fisherman	75 kg	165 cm	27.5 kg/cm ²	1580 mg	HTN
32	KS033B	M	83	Office worker	78 kg	182 cm	23.5 kg/cm ²	700 mg	DM
33	KS034B	M	78	Bricklayer	78 kg	168 cm	27.6 kg/cm ²	3900 mg	DM
34	KS035B	M	75	Farmer	82 kg	170 cm	28.4 kg/cm ²	1320 mg	DM
35	KS036B	M	69	Executive manager	75 kg	180 cm	23.1 kg/cm ²	270 mg	-
36	KS037B	M	67	Prison guard	72 kg	176 cm	23.2 kg/cm ²	870 mg	HTN
37	KS038B	M	62	Office worker	69 kg	165 cm	25.3 kg/cm ²	5200 mg	DLP, HUE
38	KS039	F	81	Housewife	86 kg	165 cm	31.6 kg/cm ²	1000 mg	HTN, HT
39	KS040	M	60	Office worker	64 kg	165 cm	23.5 kg/cm ²	2400 mg	BPH
40	KS041	M	72	Retired	78 kg	170 cm	27.0 kg/cm ²	1380 mg	DM, ASHD
41	KS043	M	76	Retired	68 kg	165 cm	25.0 kg/cm ²	800 mg	HTN, COPD
42	KS044	M	75	Businessman	62 kg	160 cm	24.2 kg/cm ²	500 mg	BLCA

Table 1. Cont.

n.	ID Sample	Sex	Age	Occupation	Body Weight	Height	BMI	Calculus Weight	Other Diseases [§]
43	KS045	M	80	Retired	75 kg	170 cm	26.0 kg/cm ²	500 mg	HTN, HUE
44	KS046	M	72	Retired	78 kg	180 cm	24.1 kg/cm ²	20 mg	DM, CRC, BLCA
45	KS047	F	50	Domestic helper	45 kg	162 cm	17.1 kg/cm ²	1300 mg	HTN, DTR
46	KS048	M	52	Office worker	78 kg	182 cm	23.5 kg/cm ²	50 mg	-
47	KS049	M	32	Unemployed	70 kg	175 cm	22.9 kg/cm ²	60 mg	-
48	KS050B	M	81	Retired	78 kg	165 cm	28.7 kg/cm ²	60 mg	BPH, HTN
49	KS051B	M	78	Retired	72 kg	165 cm	26.4 kg/cm ²	300 mg	HTN, DM

[§] Abbreviations for diseases: ASHD, arteriosclerotic heart disease; BLCA, bladder cancer; BPH, benign prostatic hypertrophy; CLC, colorectal cancer; COPD, chronic obstructive pulmonary disease DM, diabetes mellitus; DLP, dyslipidemia; DTR, dysthyroidism; GERD, gastroesophageal reflux disease; HT, hypothyroidism; HTN, hypertension; HUE, hyperuricemia; OP, osteoporosis; RF, renal failure; UC, ulcerative colitis.

Lab strategy (Table S1) was planned as a function of the availability of material that ranges from 60 mg to 9.7 g in bladder stones and from 9 mg to 2.4 g in the other urinary stones (Table 1). A preliminary morphological description of bladder stones has been carried out by means of a NIKON SMZ 1000 stereomicroscope connected to a NIKON digital Sight DSRi2 camera. Polarized light microscopy (PLM) observations carried out on thin sections (ca. 30 µm) using a Nikon Eclipse 6400 POL microscope equipped with a Nikon DS-Fi camera provided information on the microtextural features and the mineralogical composition of the bladder stones. Chemical phases were also detected by Fourier transform infrared spectroscopy (FTIR) performed in Attenuated Total Reflectance mode (ATR) by means of a Bruker ALPHA-R spectrometer (Bruker Opus 7.2 software) in the mid-infrared spectral range (4000–400 cm⁻¹, 64 scans, 4 cm⁻¹ resolution). Observations of microstructures have been made via scanning electron microscopy (SEM) on freshly fractured and gold- or carbon-coated fragments, whereas microchemical analyses on carbon-coated thin sections were performed using a Zeiss SEM EVO HD15 (Carl Zeiss, Oberkochen, Germany), operating at 20 kV accelerating voltage and 200 pA I probe current, equipped with an Oxford Instruments Microanalysis Unit (Xmax 80 EDS detector). For EDS calibrations, the Smithsonian Microbeam Standards were used [22–30].

All analytic methods were carried out in accordance with international guidelines and scientific literature [5,6,31–33]. Clinical interviews were held in anonymous form. An informed consent allowed all patients to participate in the present investigation and to publish the data in a journal article (in anonymous form). All experimental protocols were ethically approved by San Pio Hospital, according to the collaboration agreement subscribed in 2018 with the Department of Science and Technology of the University of Sannio, Benevento (Italy).

3. Results

Human urinary stones collected at San Pio Hospital were classified according to the morpho-constitutional classification proposed by Daudon et al. [6] and references therein. It is based on the description of the morphological features of both external surface and internal structure of uroliths, as well as their chemical and mineralogical composition. In particular, seven types of stones can be distinguished according, at first instance, to the main mineralogical composition: type I, whewellite (calcium oxalate monohydrate, COM); type II, weddellite (calcium oxalate dihydrate, COD); type III uric acid and urate; type IV phosphate stones; type V, cystine; type VI, protein; type VII miscellaneous stones. Further, 22 subtypes of uroliths can be distinguished as a function of their morphological features, which leads to detailed clinical assumptions about common causes and therapeutical approaches [5,6,33–35].

The results of the present investigation have been exposed and discussed in the following sections according to the main mineralogical composition of the examined uroliths, namely calcium oxalates (CaOx), uric acids (UA), calcium phosphates (CaP) and

mixed stones. The main results are summarized in Table 2, whereas Figures 1–4 display the representative microscopic and spectroscopic features of the urinary stones here analyzed.

Table 2. Morpho-constitutional classification of human urinary stones from San Pio Hospital (Benevento, Italy). * From [11]; O.M., amorphous organic matter; UA, uric acid; AU, ammonium urate; tr., traces.

n.	ID	Morphological Features			Mineralogical Composition		Type
		Surface	Internal Structure	Color	Main Phases	Minor Phases	
1	KS004	Smooth and umbilicated	Thin layers surrounding a compact concentric core	Whitish/brown	CaOx	CaP (tr.), O.M. (tr.)	Ia
2	KS010	Mamillary and umbilicated	Compact concentric, locally unorganized	Pale brown	CaOx	CaP (tr.)	Ia
3	KS030	Mamillary and umbilicated	Concentric layers	Brown	CaOx	CaP (tr.)	Ia
4	KS044	Smooth and umbilicated	Thin layers surrounding a compact concentric core	Whitish/brown	CaOx	CaP (tr.), O.M. (tr.)	Ia
5	KS045	Mamillary and rough	Compact radiating structure	Brown	CaOx	CaP, O.M.	Ia
6	KS049	Mamillary	Compact radiating structure	Brown	CaOx	CaP (tr.), O.M. (tr.)	Ia
7	KS014	Mamillary and rough	Compact unorganized	Brown	CaOx	CaP (tr.)	Ib
8	KS012B *	Sea urchin appearance	Compact concentric, locally unorganized	Dark brown	CaOx	CaP (tr.)	Ia
9	KS026	Mamillary and rough	Compact radiating and concentric, locally unorganized	Brown	CaOx	CaP (tr.)	Ia
10	KS017	-	Compact unorganized	Dark brown	CaOx	CaP (tr.), O.M. (tr.)	Ib
11	KS021	Rough	Compact unorganized	Dark brown	CaOx	UA, O.M. (tr.)	Ib
12	KS024	Mamillary and rough	Compact unorganized	Dark brown	CaOx	CaP (tr.)	Ib
13	KS027	Mamillary and rough	Compact unorganized	Brown	CaOx	CaP (tr.)	Ib
14	KS033B	Smooth, locally budding	Compact concentric, locally unorganized	Dark/pale brown	CaOx	CaP (tr.)	Ie
15	KS018	-	Compact unorganized	Pale brown	CaOx	CaP	I
16	KS025	Mamillary	Gap	Pale brown	CaOx	CaP (tr.), O.M. (tr.)	I
17	KS031	-	Compact radiating structure, poorly organized	Dark brown	CaOx	CaP (tr.)	I
18	KS051	Mamillary, loose bipyramidal crystals	Compact radiating and concentric structure	Colorless/brown	CaOx	CaP	I
19	KS001	Spiculated, bipyramidal crystals	Loose crystallization	Light brown	CaOx	CaP (tr.)	IIa
20	KS005	Spiculated, bipyramidal crystals	Loose crystallization	Light brown	CaOx	CaP, O.M. (tr.)	IIa
21	KS013	Spiculated, bipyramidal crystals	Compact unorganized	Brown	CaOx	-	IIa
22	KS048	Spiculated, bipyramidal crystals	Loose crystallization	Colorless	CaOx	CaP	IIa
23	KS028B	Spiculated, bipyramidal crystals	Compact unorganized	Pale brown	CaOx	CaP (tr.)	IIb
24	KS036B	Spiculated, bipyramidal crystals	Compact unorganized	Brown	CaOx	CaP (tr.), O.M. (tr.)	IIb
25	KS040	Spiculated, bipyramidal crystals	Compact unorganized	Brown	CaOx	CaP (tr.)	IIb
26	KS003	Smooth	Compact and concentric	Orange	UA	-	IIIa
27	KS011B *	Smooth	Compact and concentric	Pale yellow	UA	CaOx	IIIa
28	KS015	Smooth	Compact and concentric	Orange	UA	CaOx (tr.)	IIIa
29	KS016	Smooth	Compact and concentric	Orange	UA	-	IIIa
30	KS023B *	Smooth	Compact and concentric	Orange	UA	-	IIIa
31	KS029B	Smooth	Compact and concentric	Orange/Gray	UA	-	IIIa
32	KS034B	Smooth	Compact and concentric	Orange	UA	-	IIIa
33	KS035B	Smooth	Compact and concentric	Orange/Gray	UA	-	IIIa
34	KS037B	Smooth	Compact and concentric	Orange	UA	CaOx (tr.)	IIIa
35	KS038B	Smooth	Compact and concentric	Orange	UA	-	IIIa
36	KS050B	Smooth	Compact and concentric	Orange	UA	O.M.	IIIa

Table 2. Cont.

n.	ID	Morphological Features			Mineralogical Composition		Type
		Surface	Internal Structure	Color	Main Phases	Minor Phases	
37	KS022B *	Rough, embossed	Compact and concentric	Orange/Brown	UA	CaOx (tr.)	IIIa/IIIb
38	KS043	Rough	Porous and poorly organized	Brown/Orange	UA	CaOx	IIIb
39	KS020B *	Rough, porous	Concentric, locally porous, and poorly organized	Orange/Gray	UA	-	IIIb
40	KS009	Rough	Porous and poorly organized	Orange	UA	-	IIIb
41	KS046	-	-	Orange	UA	-	III
42	KS008	Rough	Loose concentric layers	Brown/whitish	Carbonated apatite	CaOx	IVa1
43	KS006B *	Rough and dappled	Concentric layers and radial crystallization	Pinkish	Brushite	CaOx, CaP	IVd
44	KS002	Rough and mammillary	Unorganized	Brown	UA/CaOx	CaP (tr.)	IIIb/Ia
45	KS039	Smooth and mammillary	Alternated orange concentric layers and brown compact radiating levels	Orange/dark brown	UA/CaOx	CaP (tr.)	IIIa/Ia
46	KS007	Mammillary and locally spiculated	Thin concentric layers surrounding an unorganized core	Pale brown	CaOx/CaP	-	Ia/IIb/IVa
47	KS047	Mammillary and locally spiculated	Locally compact, concentric layers	Pale brown	CaOx/CaP	-	Ia/IIb/IVa
48	KS032B	Rough, spiculated	Unorganized		CaOx/CaP	-	IIa/IVa
49	KS041	Rough	Unorganized layer surrounding a compact core with radiating crystallization	Grayish/dark brown	AU/CaOx	CaP (tr.)	IIIc/Ia/IIb

3.1. Classification of Uroliths and Etiology

3.1.1. CaOx Stones

Twenty-five (25) examined urinary stones are made of calcium oxalate (CaOx) as dominant mineral phase, often accompanied by minor uric acids (UA), calcium phosphates (CaP) and organic matter (Table 2). Between them, only 4 (KS012B, KS028B, KS033B and KS036B) were bladder stones, whereas the remaining 2121 samples came from kidney. Mineralogical composition of these samples was highlighted by FTIR measurements, and their morphological features are consistent with literature [6]. In particular, FTIR spectra of CaOx stones are characterized by a sequence of broad and very weak absorption bands located at around 3432 cm^{-1} , 3331 cm^{-1} , 3240 cm^{-1} and 3050 cm^{-1} (symmetric and asymmetric O-H stretching vibrations), followed by sharp and very strong diagnostic bands at ca. 1612 cm^{-1} (C=O vibration), 1314 cm^{-1} (C-O vibration), 779 cm^{-1} (C-H bending), 513 cm^{-1} (in plane O-C=O bending) (Figure 4 and Table S2a).

Whewellite (ideal composition $[\text{CaC}_2\text{O}_4 \cdot \text{H}_2\text{O}]$) and weddellite (ideal composition $[\text{CaC}_2\text{O}_4 \cdot (2+x)\text{H}_2\text{O}]$, where $x < 1$) [36–38] are the most common calcium oxalate phases occurring in human urinary stones and are classified, according to the literature [5,6], as type I and type II, respectively. The strong intensity of the diagnostic FTIR bands observed at about 779 and 513 cm^{-1} for most of the analyzed CaOx samples is generally indicative of the presence of whewellite, the most stable calcium oxalate phase. Conversely, samples KS001, KS028B, KS036B and KS048 shows a significant low absorbance intensity for these two bands that would suggest the occurrence of weddellite as dominant mineralogical phase. Nevertheless, only FTIR measurements could not fully discriminate between these two biominerals when they occur as mixtures or not in pure form, although a first discrimination may be provided by an accurate micro-morphological observation of both internal and external parts of the calculus. The best analytical method to distinguish these oxalates is doubtless X-ray diffraction (XRD) since it highlights the different crystallographic features of whewellite (monoclinic, P21/c) and weddellite (tetragonal, I4/m) [39]. However, FTIR still represents the most common spectroscopic technique used for stone analysis as it

provides very useful information for clinical purposes by means of a less expensive and time-consuming approach, and requiring very low amounts of biominerals (<10 mg) [40].

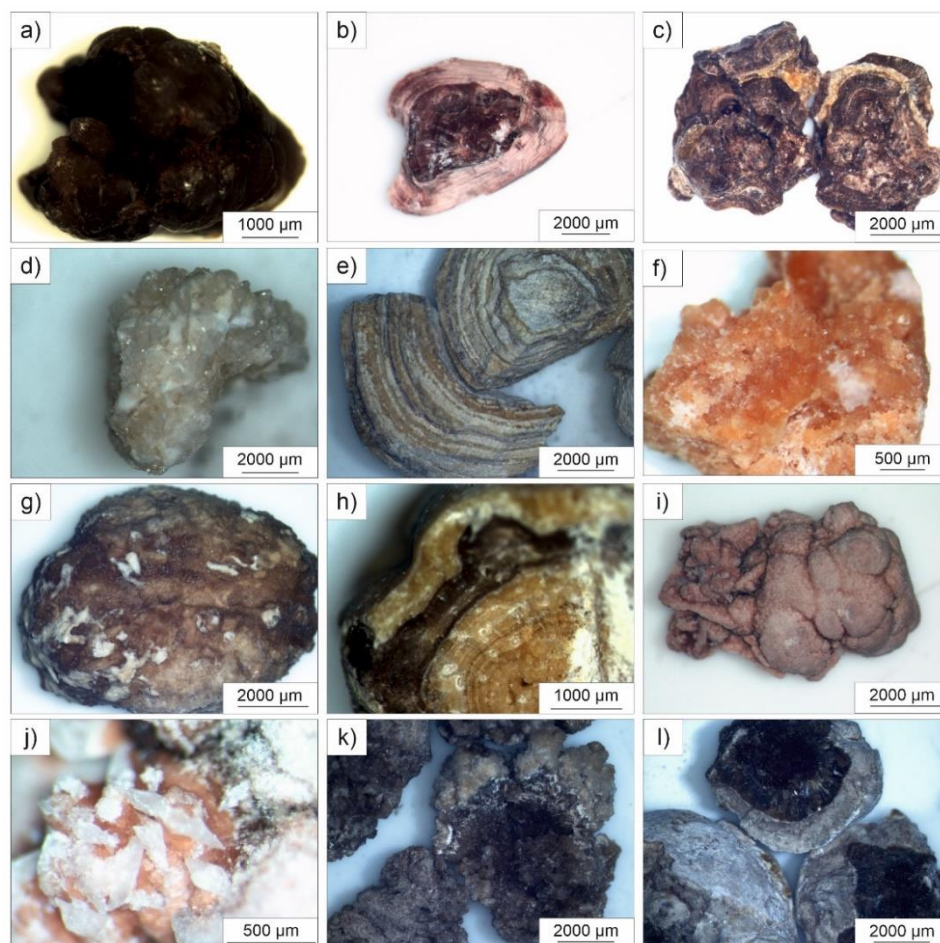


Figure 1. Micrographs of urinary stones captured in stereomicroscopy: (a) mammillary, dark brown type Ia calculus (KS049); (b) whitish thin layers of CaOx surrounding a compact concentric, dark brown core with radiating crystallization (KS004); (c) dark brown, compact unorganized type Ib calculus (KS021); (d) colorless, spiculated type IIa urolith (KS048); (e) orange/gray uric acid stone KS035B showing concentric structure (type IIIa); (f) orange uric acid stone fragment (KS003); (g) rough, brown surface of sample KS008 (carbonated apatite); (h) layers of uric acid and CaOx in sample KS039; (i) complex external morphology of mixed stone KS007; (j) bipyramidal, colorless crystals of weddellite in sample KS007; (k) rough and spiculated surface with unorganized internal section of bladder stone KS032B; (l) ammonium urate layer surrounding a compact core of CaOx with radiating crystallization in sample KS041.

The color and the inner structure of CaOx stones mainly depends on the kinetics of crystals growth. A well-organized structure derives from a slow minerogenetic process that leads to the formation of compact concentric layers and radiating crystallization, during which pigments from urine can be easily incorporated in the lattice of CaOx biominerals conferring the typical brownish color of COM (type I) (Figure 1a–c). On the contrary, a rapid crystallization results in colorless or lighter colored aggregates with unorganized structures (COD, type II) (Figure 1d).

In type I, whewellite usually shows a mammillary, budding, smooth, or slightly rough surface, whereas type II urinary stones generally appear with spiculated surfaces with recognizable bipyramidal crystals of weddellite (or pseudomorphic whewellite (Gibson 1974)). Normally, crystallization of CaOx stones is attributable to hypercalciuria (i.e., COD) and/or hyperoxaluria (i.e., COM). Rarely, especially due to specific drug intake, an unstable

calcium oxalate trihydrate (COT, caoxite) has been observed [41,42]. Apart from hyperoxaluria and hypercalciuria, CaOx stones formation could be due also to hyperparathyroidism or other metabolic dysfunctions [5].

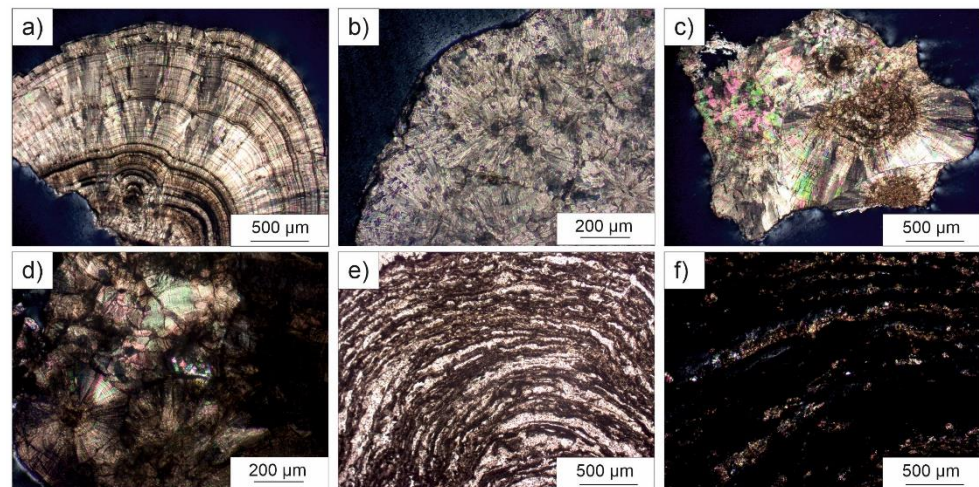


Figure 2. Micrographs of urinary stones captured in polarized light microscopy: (a) compact radiating and concentric internal structure in CaOx kidney stone KS026 subtype Ia (crossed polars, CP); (b) compact unorganized internal structure of subtype Ib sample (KS014, CP); (c) unorganized internal structure of CaOx sample KS031; (d) subtype IIb sample (KS013) with residual organic matter; (e,f) loose concentric layers of carbonated apatite and CaOx in sample KS008 (subtype IVa1), in plane and crossed polars, respectively.

According to the results summarized in Table 2, most of these samples generally show the typical surface of type I calculi. As a whole, the color of both surface and internal structure ranges from pale to dark brown. The ones with a compact unorganized internal structure and a mammillary/rough surface are classified as subtype Ib (Figure 2b,c). This category is often considered idiopathic although observed in patients suffering urine stasis, and are sometimes due to a progressive conversion of COD to COM [6].

Samples KS010, KS026, KS030, KS045, and KS049 are characterized by the occurrence of frequent umbilications on their mammillary surfaces. This feature, along with a compact radiating and concentric internal structure, allow classifying them as subtype Ia (Figure 2a), a category of kidney stones with peculiar minerogenetic mechanisms. In particular, umbilication (also known as papillary imprint) consists in a small depression (Figure 3a,b) representative of the contact with the renal papilla, by means of a calcium phosphate deposit known as Randall's plaque [43–47]. Formation of type I calculi is generally related to dietary habits as, for example, an excessive intake of oxalate-rich foods, low water intake, and low diuresis. Worth to note is that a low calcium intake could lead to the crystallization of whewellite aggregates since the in excess oxalate ions can be easier sorbed by the organism.

Morphological features of samples KS004 and KS044 are quite interesting as they are characterized by thin whitish layers surrounding a brown compact concentric core (probably a fragment of a subtype Ia). The external whitish layers should be due to the rapid crystallization of whewellite on the surface of a pre-existing darker fragment.

Euhedral bipyramidal and colorless crystals of weddellite affect the mammillary surface of sample KS051, which displays a compact radiating and concentric internal structure, brown in color.

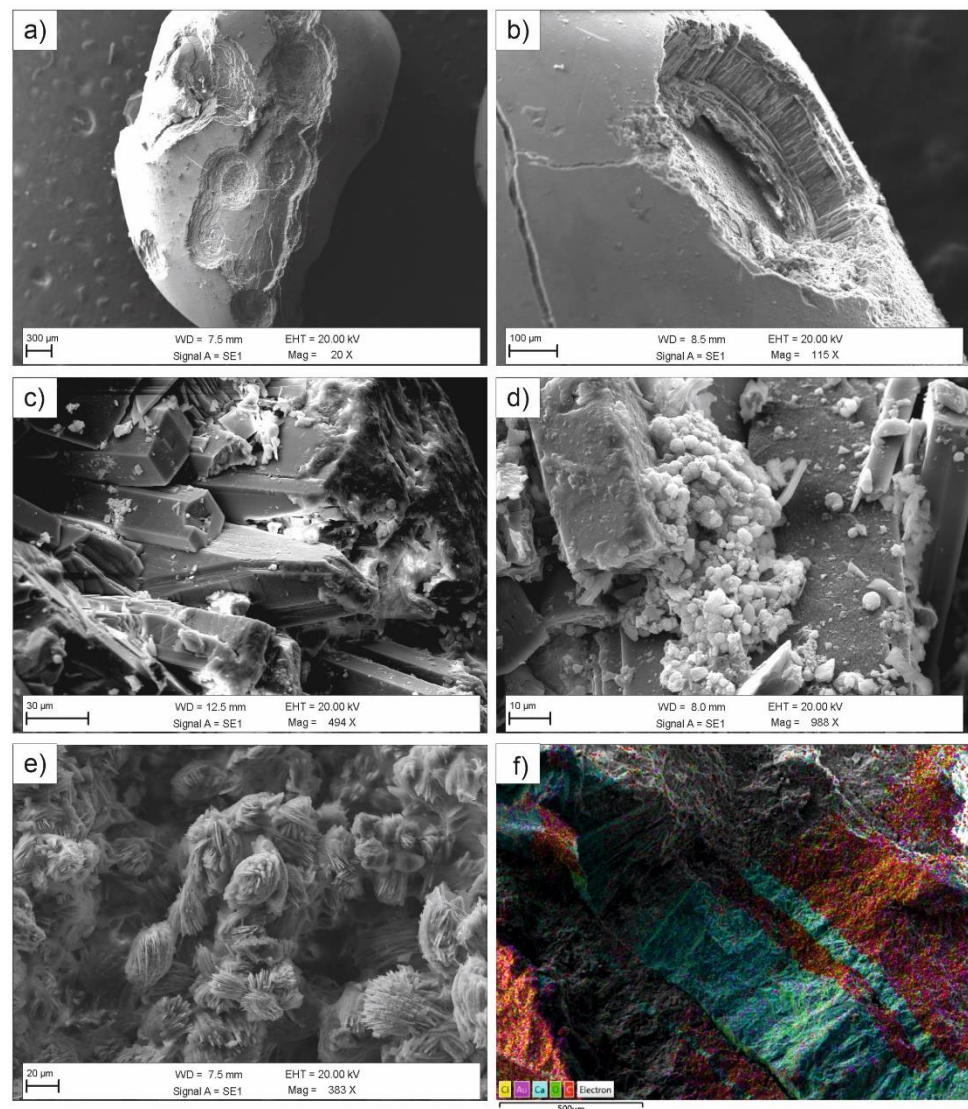


Figure 3. Secondary electron images of the examined calculi: (a,b) umbilicated surface of sample KS044 (subtype Ia); (c) prismatic crystals of brushite (subtype IVd) with (d) spheroidal inclusions of CaP stones in the porous system; (e) weddellite aggregates showing a “desert rose” shape in a mixed urinary stone (KS041, type VII); (f) distribution of Ca and C in alternated layers of uric acids and CaOx in sample KS039 (subtype IIIa/Ia).

KS033B shows a compact radiating, concentric structure, locally unorganized with a smooth budding surface. These features are quite consistent with those of subtype Ie. This kind of calculus is not frequent but clinically relevant as it can be attributed to enteric hyperoxaluria or type 2 diabetes. Actually, during the clinical interview patient KS033B stated to suffer from diabetes mellitus (Table 1).

The absence of specific features (probably lost during surgical extraction) in the remaining type I calculi cannot allow a reliable classification, in terms of subtype, of these CaOx kidney stones.

Type II samples here examined are formed by two bladder and five kidney stones (Table 2). They are generally recognizable thanks to the speculated external surface, showing light colored or colorless bipyramidal crystals of weddellite (Figure 1d). If these crystals exhibit sharp angles and edges can be classified as subtype IIa, whereas subtype IIb calculi are characterized by smooth and long bipyramidal crystals. As aforementioned, COD crystals form in patients with idiopathic hypercalciuria and negligible or moderate hyperoxaluria. Nevertheless, from a mineralogical point of view, weddellite is unstable and

easily converts, by a partial dehydration, in whewellite [39,48,49]. During this transformation, whewellite often preserves the initial crystal habit of weddellite (pseudomorphism) but calcium content increases from ca. 24 wt.% (weddellite) to ca. 27 wt.% (whewellite). Sample KS013 (Figure 2d) is a typical example of this transformation inasmuch EDS analyses (Table S3) report calcium concentrations ranging between 24.2 and 28.7 wt.% from the outer to the inner portion of the kidney stone. Furthermore, crystals on the external surface appear interested by intense cracking probably due to an initial dehydration stage of weddellite. Worth to note is also the occurrence of phosphorous (0.26 ± 0.1 wt.%) and sulfur (0.24 ± 0.1 wt.%) as minor elements, likely deriving from residual organic matter and crystallization of calcium phosphate.

The dry conditions of the more compact inner parts of the bladder stones, likely enhance a dehydration of calcium oxalates up to the formation of an anhydrous phase CaC_2O_4 , stoichiometrically characterized by a calcium content of ca. 31.0 wt.% [11]. This could be observed, for example, in sample KS028B where ranges from 26.9 to 31.6 wt.%. A similar result was reported by Mercurio et al. [11] for the innermost part of the bladder stone KS012. Although synchrotron X-ray diffraction showed the only presence of whewellite. Actually, calcium oxalate is a highly hygroscopic substance and its anhydrous form (calcium oxalate anhydrous, COA) consists of three polymorphs (α -COA, β -COA, γ -COA) obtained by dehydration of weddellite [50]. Unfortunately, information about framework and polymorphism of COA is still controversial but Hocart et al. [51] considered the dehydration of whewellite essentially topotactic with no significant structural rearrangement for α - and β - phases. Nevertheless, without conclusive crystallographic evidence, any hypothesis here proposed about the presence and formation mechanisms of COA need further specific investigations.

As observed for KS013, also KS028B shows traces of phosphorous (0.1 ± 0.04 wt.%) and sulfur (0.1 ± 0.01 wt.%), along with chloride (0.1 ± 0.07 wt.%). These trace elements were already observed in human urinary stones in other investigations [52,53].

3.1.2. Uric Acids

Sixteen samples of the examined urinary stones consist of uric acid, mainly coming from bladder (Table 2). According to the literature, uric acid stones (type III) can be distinguished in two subtypes: a first one (subtype IIIa) made of anhydrous uric acid (ideal composition $[\text{C}_5\text{H}_4\text{N}_4\text{O}_3]$) and a second one (subtype IIIb) where uric acid dihydrate $\text{C}_5\text{H}_4\text{N}_4\text{O}_3 \cdot 2\text{H}_2\text{O}$ is the predominant biomineral.

In the present investigation, most of the analyzed uric acid stones are classified as subtype IIIa as characterized by a compact, concentric, and radiating crystallization along with a smooth surface (Figure 1e). On the other hand, only kidney stones KS009 and KS043 and the bladder stone KS020B display a rough and porous surface, with poorly organized inner structure, typical of subtype IIIb.

FTIR pattern of uric acid stones is characterized by the occurrence of a dense sequence of narrowed absorption bands in the spectral range $1800\text{--}400\text{ cm}^{-1}$, the fingerprint region (Figure 4 and Table S2b) [54]. At higher wavenumbers, it is possible to observe a broader band between 3300 and 2800 cm^{-1} , from which arise some diagnostic signals at ca. 3088 cm^{-1} , 2995 cm^{-1} , 2917 cm^{-1} , 2792 cm^{-1} , 2690 cm^{-1} , and 2605 cm^{-1} generally attributable to N-H stretching vibrations [55,56]. In three samples (KS015, KS037B and KS050B), traces of organic matter and/or calcium oxalates were also detected (Table S2b).

This type of urolith shows an orange color due to the presence of uricine, a pigment of urine that can be trapped into the uric acid crystals. The color of uricine is pH-dependent and can shift from reddish-yellow to green in acidic environment [57]. In uric acid stones this pigment confers an orange color to the urolith, especially in the more stable mineralogical phase (uricite) belonging to subtype IIIa (Figure 1f). As already noted for CaOx uroliths, even uric acids undergo to a spontaneous dehydration process that leads to the stabilization of the subtype IIIb in the more stable anhydrous phase subtype IIIa, often retaining the initial IIIb morphology. This phenomenon was clearly observed by Mercurio et al. [11] in

bladder stone KS022B that shows both the internal concentric structure of subtype IIIa and the rough and embossed external surface of subtype IIIb.

The uric acid nephrolithiasis is usually attributable to eating and metabolic disorders, stasis, hyperuricosuria, and low pH urine. Subtype IIIa are typically observed in older patients affected by prostate hypertrophy whereas diabetes is often one of the common causes for the formation of subtype IIIb [5].

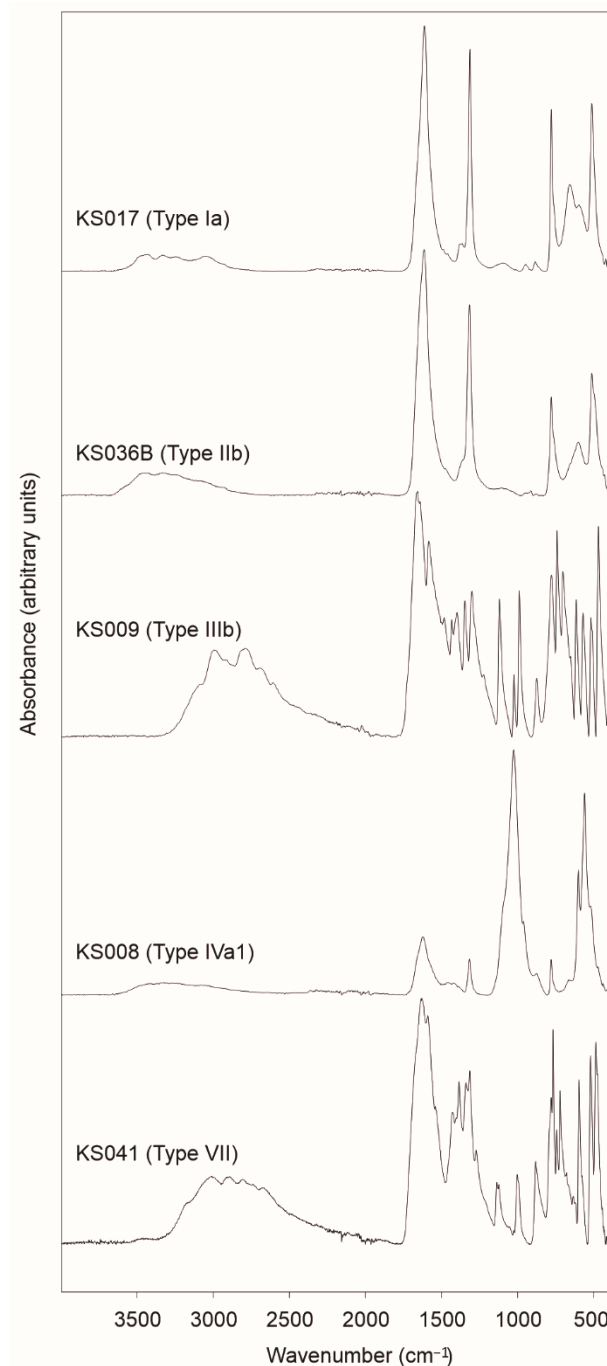


Figure 4. Representative FTIR spectra of the examined uroliths: whewellite in sample KS017 (type Ia); weddellite in bladder stone KS036B (type IIb); uric acid in sample KS009 (type III); carbonated apatite in sample KS008 (type IVa1); ammonium urate and calcium oxalate in mixed stone KS041 (type VII).

3.1.3. CaP Stones

Samples KS006B and KS008 are the only two uroliths belonging to the calcium phosphate stones (type IV). Mercurio et al. [11] classified KS006B as a subtype IVd since mainly formed by brushite (ideal composition $[\text{CaHPO}_4 \cdot 2(\text{H}_2\text{O})]$), along with minor CaOx and CaP crystals, showing a rough and dappled surface, and a concentric layers structure with radial crystallization. At SEM, it is clearly observable the tabular shape of brushite crystals and the occurrence of spheroidal or acicular CaP inclusions mainly located into the porous internal structure (Figure 3). This kind of calculus is usually considered as idiopathic, although it is often observed in patients affected by primary hyperparathyroidism and hypercalciuria [5] and renal phosphate loss [8]. The detection of brushite is meaningful from a clinical point of view due to the fact that it represents a biomineral very resistant to the fragmentation by means of extracorporeal shock wave lithotripsy (ESWL) and characterized by a high recurrent rate [58,59].

KS008 shows a rough brown surfaces and loose concentric layers in the internal section (Figures 1g and 2e,f). This calculus is the only urinary stone mainly composed by carbonated apatite layers alternating minor levels of CaOx (subtype IVa1). Carbonated apatite (ideal composition $[\text{Ca}_{10}(\text{PO}_4\text{CO}_3)_6(\text{OH})_8]$) consists in a hydroxyapatite interested by variable substitutions of carbonate ion CO_3^{2-} in the place of phosphate ion PO_4^{3-} (B-type substitution) or, less frequently, OH^- group (A-type substitution) [60,61]. According to the literature [56,62–65], FTIR pattern of the carbonated hydroxyapatite here examined (Figure 4 and Table S2c) is characterized by a very strong absorption band at ca. 1026 cm^{-1} representative of the antisymmetric stretching vibration of phosphate ion ($\nu_3 \text{PO}_4^{3-}$) along with a shoulder at ca. 962 cm^{-1} (symmetric stretching $\nu_1 \text{PO}_4^{3-}$), and other narrow and strong diagnostic bands at ca. 601 and 561 cm^{-1} generally attributable to the bending vibrations $\nu_4 \text{PO}_4^{3-}$. The weak bands around 1461 and 1421 cm^{-1} refer to antisymmetric stretching vibration of carbonate ion ($\nu_3 \text{CO}_3^{2-}$), whereas the band at ca. 878 cm^{-1} is attributable to the out-of-plane bending ($\nu_2 \text{CO}_3^{2-}$). Lastly, a broad band at ca. 3290 cm^{-1} also occurs.

Mineral composition of the urinary stone belonging to subtype IVa can provide important information about etiology. Generally, subtype IVa1 derives from patients affected by hypercalciuria and/or urinary tract infection (UTI). Nevertheless, further information rises from the carbonation ratio $[\text{CR} = (\nu_3 \text{CO}_3^{2-})_{\text{Abs}} / (\nu_3 \text{PO}_4^{3-})_{\text{Abs}}]$ [6,40,66]. For example, a high CR value (generally $> 15\%$) is indicative of a UTI induced by urease-producing bacteria, especially in presence of struvite (ideal composition $[(\text{NH}_4)\text{MgPO}_4 \cdot 6(\text{H}_2\text{O})]$) [67]. On the other hand, lower CR values, in absence of struvite, are usually attributable to hypercalciuria without urinary tract infections. CaP stone KS008 shows a CR of ca. 5% combined to the presence of CaOx phases with a Ca content of ca. 26.2 wt.% (Table S3). Therefore, in absence of struvite or other compounds such as, for example, whitlockite (ideal composition $[\text{Ca}_9\text{Mg}(\text{PO}_4)_6(\text{PO}_3\text{OH})]$), the formation of KS008 calculus is probably due to hypercalciuria without UTI, as also inferable by the absence of bacteria imprints that could be observed in SEM for these kind of urinary stones [21,40]. Lastly, EDS analyses show the occurrence in this carbonated apatite of trace elements such as sodium ($0.82 \pm 0.16 \text{ wt.}\%$), magnesium ($0.75 \pm 0.17 \text{ wt.}\%$), zinc ($0.18 \pm 0.01 \text{ wt.}\%$) and chloride ($0.24 \pm 0.10 \text{ wt.}\%$). Trace elements can be easily found in CaP as consequence of the several isomorphic substitutions characterizing these mineralogical phases [11]. Note that the undetermined composition of biological apatite is largely discussed in the literature as nonstoichiometric and with variable Ca:P ratio and carbonate ions contents [68]. In fact, the above mentioned ideal composition of carbonated (hydroxy)apatite (often called carapatite by urologists) is a canonical expression far from the real composition that can be better represented as $\text{Ca}_{10-x+u}\square_{x-u}(\text{PO}_4)_{6-x}(\text{CO}_3)_x(\text{OH})_{2-x+2u}\square_{x-2u}$ where $0 < x < 2$, $0 < u < x$ and the squares correspond to vacancies or additional cations and anions [40].

3.1.4. Mixed Stones

Urinary stones are usually composed by a dominant mineralogical phase along with additional compounds that occur as minor or trace components. However, if the uroliths present more than one main mineralogical phase, it can be classified as type VII (miscellaneous), where color and morphological features of both surface and internal structure depend on the its actual chemical and mineralogical composition (Daudon et al. 2016). In the present investigation, five kidney stones (KS002, KS007, KS039, KS041, KS047) and 1 bladder stone (KS032B) belong to this category.

Samples KS002 and KS039 are both composed by a mixture of uric acid and CaOx crystals, as demonstrated by FTIR analyses (Figure 4 and Table S2d). Nevertheless, these samples are quite different from a morphological point of view: the former displays a mammillary and rough brown surface with an unorganized internal structure (subtype IIIb/Ia); the latter are characterized by smooth and mammillary surface with an internal structure made of alternated orange and concentric layers of uric acids and compact and radiating brown level of CaOx (subtype IIIa/Ia) (Figures 1h and 3f). This kind of nephrolithiasis is frequent and severe [69], especially in obese patients affected by hyperoxaluria and metabolic syndrome. As confirmed by clinical interview (Table 1), both patients KS002 and KS039 are considered obese since their BMI is over 30 Kg/cm². Furthermore, patients state to suffer of dyslipidemia (KS002) and HTN (KS039).

According to FTIR results (Table S2d), KS007, KS032B, and KS047 consist in mixtures of CaOx and CaP crystals. Surfaces of KS007 and KS047 are mammillary and locally spiculated, with frequent colorless bipyramidal crystals of weddellite (Figure 1i,j). The section of KS007 is characterized by thin concentric layers surrounding an unorganized nucleus (Figure 2), whereas KS047 by locally compact concentric layers. On the other hand, sample KS032B shows a very rough spiculated surface with an unorganized internal section interested by white CaP thin layers (Figure 1k).

CaOx/CaP association in uroliths is often idiopathic, although some connections with specific etiologies have been reported [70–74].

Particular attention should be paid to KS041 sample. This urolith is composed by a thin grayish layer surrounding a brown compact nucleus showing a radiating crystallization (Figure 1l). As inferred by FTIR analysis (Figure 4 and Table S2d), KS041 is mainly formed by ammonium urate (ideal composition [NH₄C₅H₃N₄O₃]) and calcium oxalates. Although similar to uricite from a spectroscopic point of view, FTIR pattern of ammonium urate displays some additional diagnostic signals at ca. 1540 cm⁻¹, 1273 cm⁻¹, 1003 cm⁻¹, 768 cm⁻¹, 722 cm⁻¹ and 597 cm⁻¹ [56]. In this sample, ammonium urate (subtype IIIc) envelops a nucleus consisting in a fragment of a whewellite urolith (subtype Ia) probably caused by a urinary tract infection. SEM observations clearly show the occurrence of weddellite aggregates with a “desert rose” shape (Figure 3e). Usually, this nephrolithiasis occurs in urines with high pH values after their therapeutic alkalinization [5,6].

3.2. Distribution and Risk Factors

One of the most recent epidemiological investigations on stone disease across the world was reported by Sorokin et al. [75] in 2017. The authors stated that the prevalence of urolithiasis ranges from 1% to 5% in Asia, 7% to 13% in North America, and 5% to 9% in Europe, with a rising incidence from the 2007 [76] to the 2017 followed by a narrowing of the sex gap. Nevertheless, epidemiology of urolithiasis can vary significantly within the single countries [77]. For example, in USA the prevalence gradually increased (3.8% between 1976 and 1980, 5.2% between 1988 and 1994, and 8.8% between 2007 and 2010) [78,79]. In great continents such as Asia the prevalence of urolithiasis can significantly change: from 1% in Iraq [80] up to 19.1% in Saudi Arabia [81].

The prevalence of urolithiasis in Italy also increased in the last decades (ca. 1.17% in 1983 and 1.72% in 1993–1994) [75]. Unfortunately, as far as we know, there are not recent epidemiological studies about stone disease that completely cover the Italian territory. Nevertheless, Prezioso et al. [3] carried out in 2014 an accurate statistical investigation on

a population of 900,994 patients living in all Italian regions before 31 December 2012, in which data were collected on the Health Search/CSD Longitudinal Patient Database (HS) used by Italian Society of General Medicine (SIMG). The authors noticed a prevalence of ca. 4.13%, higher in males than in females. These values can vary significantly between regions. In this frame, Campania region showed the highest value (ca. 6.08%).

Other investigations give further information about the prevalence of urolithiasis within provinces and single cities. For example, Trinchieri et al. [3] observed, for patients older than 25 years from Milan (Lombardy, northern Italy), a prevalence of ca. 5.6% in 1986 and 9.0% in 1998. As noticed by a significant statistical investigation carried out by Croppi et al. [2] on selected Caucasian adult subjects during January–May 2011, the prevalence of this disease in Florence (Tuscany, central Italy) was ca. 7.5%. These values are quite consistent with the epistemological data reported in the guideline on urinary stones edited by the Association of Italian Urologists [82] (and references therein) where an incidence of ca. 100,000 new cases each year has been observed.

Urolithiasis often represents an important cause of admission in Italian emergency departments, although a significant reduction in the number of admitted patients was attested after the national lockdown at the beginning of March 2020, especially for those cities, such as Rome, where hospitals were mainly devoted to the management of COVID-19 pandemic [1]. The same occurred for the Department of Urology of the San Pio Hospital (Benevento, Italy). Therefore, most of the uroliths here examined were collected before the national lockdown. Actually, during COVID-19 pandemic a very little number of samples was extracted from patients admitted for a real emergency related to stone disease, often interesting the bladder. In fact, the European Association of Urology considered bladder stones responsible for ca. 8% of urolithiasis-related mortalities in developed nations [32].

The results of the present study just enable a first and preliminary comparison (Table 3) between the frequency distribution of the mineralogical composition of uroliths from the Campanian region with other investigations across the world. However, it is a matter of fact that the analysis of 49 urinary stones cannot provide a reliable and exhaustive representation of urolithiasis in a complex and multifactorial territory such as the Campania region, especially when compared to a high variable number of samples such as those reported in the considered case studies (from 25 samples for Iraq [17] to 27,980 samples for France [83]).

Nevertheless, the results of the present study just allow a first and preliminary comparison (Table 3) between the frequency distribution of the mineralogical composition of uroliths from Campanian region with other investigations across the world. First of all, except for southern Iran [19] and Japan [84,85], oxalate represents the main mineralogical phase of the human uroliths and the percentage of oxalates in Campanian region (ca. 51%) is quite comparable to those of Basilicata region [12] and other Mediterranean countries such as France [83], Spain [86], Jordan [16] and Algeria [56]. However, the higher percentages were found for northern Iran [87], China [88,89] and Democratic Republic of Congo [90–92]. Furthermore, Campania and Basilicata regions display the lowest percentage of phosphate stones (4–5%) along with Iran and Jordan, whereas it is significantly higher for other countries such as Iraq [17] and Japan [85]. Nevertheless, the frequency of purines in Campanian region is the highest ever observed (ca. 33%) (Table 3).

Prevalence and incidence of urolithiasis, as well as compositional frequency distribution of uroliths can be discussed as a function of both dietary (fluid and food intakes) and non-dietary (age, sex, climate, environment, etc.) factors.

3.2.1. Demographics and Environment

Urolithiasis is doubtless a multifactorial process, but there is a clear age and sex dependence on the urinary stone formation and composition of these pathological biominerals [18]. Although stone disease is not exclusive in adults [93,94], lifetime prevalence generally increases with age, following a rise-to-fall pattern indicating a decreasing incidence for older patients as a result of preventive measures [75,95]. In our investigation, the

highest prevalence was observed for patients over 50 years (ca. 84%), displaying the same frequency of oxalates and uric acids, along with phosphates and most of the mixed stones (Table 3). In younger individuals (24–50 years old), uroliths were quite completely made of calcium oxalate. This distribution is well consistent with the national trend [82].

Table 3. Frequency of the compositional distribution of urinary stones in patients from the Campanian region compared to literature data. Sex ratios (male-to-female) have also been reported. Note: Ox., oxalate stones; Ph., phosphate stones; Pur., purine stones; §, present study.

n.	Country/Locality	Year	N. of Stones	Ox. (%)	Ph. (%)	Pur. (%)	Others (%)	Sex Ratio	Ref.
1	Italy, Campania	2018–2019	49	51.0	4.1	32.6	12.2	6.00	§
2	Italy, Basilicata	2007–2008	80	59.0	5.0	18.0	18.0	1.27	[12]
3	France	1976–2001	27,980	65.2	18.3	9.4	7.1	2.28	[83]
4	Spain, Balearic Islands	-	700	63.1	11.8	8.2	16.9	-	[86]
5	Iran, Fars	2013	83	30.8	5.1	30.8	33.3	2.19	[19]
6	Iran, Ardabil	2001–2006	1268	80.3	0.4	18.6	0.7	2.66	[87]
7	Iraq	1997	25	46.1	38.4	15.4	-	4.00	[17]
8	China	2003–2012	12,846	78.3	18.0	3.6	0.2	-	[89]
9	Japan	2005	11,650	43.8	49.2	3.8	3.1	-	[85]
10	Jordan, Irbid City	2004–2005	135	60.0	-	6.7	33.3	1.04	[16]
11	Russia	1980–2008	750	66.0	20.8	10.5	2.7	1.90	[96]
12	Democratic Republic of Congo	2010–2018	62	72.7	13.6	12.9	0.8	1.41	[90]
13	Algeria, El Bayadh district	-	-	58.1	25.8	12.9	3.2	-	[56]
14	Korea	2009	-	-	-	-	-	1.80	[97]
15	Italy, Milan	1986; 1998	-	-	-	-	-	1.40; 1.74	[4]

According to the literature [75], the sex ratio (male-to-female) across the world (Table 3) generally ranges between 1.5 and 2.5, with some peculiar exceptions such as, for example, Jordan (ca. 1.04) and Iraq (ca. 4.0) [16,17]. This range is quite consistent with the prevalence of urolithiasis in Italy [3], although local sex disparities can be observed [2–4,12]. In our research, the sex ratio (ca. 6.0) also suggests a clear male predominance, especially for older patients (>50 years old). Nevertheless, it must be considered that this ratio was influenced by the high number of bladder stones collected (ca. 33%), usually observed in European men (sex ratio 10:1) [32] and normally extracted surgically after proper admission in urological departments.

Non-dietary factors such as for example climate and exposure to a polluted environment can be responsible for the prevalence, incidence, and recurrence of stone disease. Climate-related urolithiasis is well documented [98]. Stone formation is often favored in countries or regions characterized by warm or hot climates. For example, urolithiasis in Italy is more evident in southern regions as a consequence of the exposure of stone formers to warm and dried summers typical of the Mediterranean area [3]. In fact, the patients from San Pio Hospital stated in the clinical interviews that suffering from stone disease, mainly during the summer in the Benevento area, has been characterized in the last years by an average temperature never below 22 °C (diurnal temperature range up to 12 °C) and precipitation between 0 and 4 mm/month [99]. The occupation of patients can emphasize the exposure of the individuals to hot and/or polluted environments. About 26% of the patients from San Pio Hospital stated to have a job with heat exposure (e.g., farmers, bricklayers, cooks, etc.), leading to dehydration conditions. The exposure could also interest polluted environments or workplaces with consequent adsorption of undesired substances. In fact, a recent investigation [11] demonstrates the occurrence in the bladder stones KS006B, KS011B, KS012B, KS020B, KS022B, and KS023B of undesired and dangerous elements such as Hg, Pb, As, Cd, Cu, and Cr that, along with other trace elements, can act as promoters of stone formation or lead to more severe health consequences [53,100–102].

3.2.2. Comorbidities, Lifestyle, and Dietary Habits

Overweight and obesity play a fundamental role in stone formation, facilitating calcium excretion, the main promoter element of urolithiasis [102,103] responsible for the formation of Ca stones (both oxalates and phosphates) as predominant or minor mineralog-

ical phases (Table 2). According to the World Health Organization, ca. 63% of the patients in the present investigation were considered overweight (55%) or obese (8%) as they presented a body mass index (BMI) equal to or greater than 25 Kg/cm². The remaining patients were normal (33%, 18.5 Kg/cm² ≤ BMI ≤ 24.9 Kg/cm²) or rarely underweight (4%, BMI < 18.5 Kg/cm²) (Table 1).

Patients suffering from diabetes were about 20% and are mainly overweight and uric acid formers. This metabolic disorder represents an important risk factor in stone disease and is mainly related to the formation of uric acids due to the lower pH of urine as a consequence of insulin resistance [75,78]. Uric acid is also associated with eating and/or metabolic disorder. In fact, being mainly composed of uric acids, bladder stone formation in older men from the Campanian region could be related to an incorrect lifestyle and dietary habits.

A similar percentage of patients also stated to suffer from HTN, which is considered a risk factor as well [78,104]; nevertheless, no clear correlation has been observed as a function of the mineralogical composition of uroliths.

Benign prostatic hypertrophy and bladder cancer significantly engrave on secondary bladder stone formation since they cause obstruction of the lower urinary tract and consequently prolonged stasis of urines in the bladder. However, only 8% of the patients declared to suffer from one of these conditions (Table 1).

Arteriosclerotic heart disease was another comorbidity noticed by clinical interviews (ca. 8%) (Table 1). According to Reiner et al. [105], arteriosclerosis could share several risk factors with nephrolithiasis, whereas Luo et al. [106] consider urolithiasis as a potential risk factor for atherosclerosis. Additional diseases declared during clinical interviews are reported in Table 1.

Apart from risk factors related to inheritance and genetics, often responsible for common idiopathic calcium oxalate stone formation [75], some risk factors could be avoided by pursuing a correct lifestyle and dietary habits [107].

For example, arterial HTN and obesity can be contrasted by regular physical activity and consumption of a dietary approach to stop HTN (DASH-style diet) [108]. However, only 10% of the patients stated during the clinical interview that to have regular physical activity. Furthermore, about half of the patients are retired, have a desk job, or are housewives (Table 1). Epidemiological questionnaires also reported a constant consumption of alcohol by most of the patients along with the consumption of protein- and oxalates-rich foods (such as for example coffee, cocoa, dried fruit, meat, eggs, cheese, etc.) that normally cause a supersaturation of urines and consequent pathological biomineralization in the urinary tract (especially in the bladder) in the form of uricite (type III) and whewellite/weddellite (types I and II). Drinking water quality also plays an important role in urolithiasis, especially when characterized by a high calcium content or generally high total dissolved solids (TDS). The most important aquifers in continental Southern Italy (including the Campanian region) are hosted by meso-Cenozoic carbonate platform complexes [109]. Therefore, hydrogeological resources provided by these aquifers and distributed as tap water are normally characterized by significant amounts of calcium or other ions that usually promote urolithiasis. For this reason, most stone formers are wary of consuming tap water, preferring to drink bottled water (often with the same or worse physicochemical parameters). In fact, only four patients from San Pio Hospital stated to drink exclusively tap water. The mistrust about the quality of tap water is often unfounded since urolithiasis can usually be due to a not regular fluid intake and proper diuresis [110].

4. Conclusions

The importance of a proper compositional and morphological analysis of stones coming from human pathological biomineralization is strongly highlighted in several international guidelines and scientific papers concerning the treatment of urolithiasis [31–33]. For example, Pearle et al. [31] clearly stated, as a clinical principle, that “When a stone is available, clinicians should obtain a stone analysis at least once” and “Clinicians should obtain

a repeat stone analysis, when available, especially in patients not responding to treatment". In fact, knowledge of stone composition may directly help preventive measures and plan proper therapeutical approaches, providing a valuable contribution to the management of pathological biomineralization at a regional scale.

This investigation demonstrates how a methodological approach based on the use of conventional analytical techniques may lead to a complete morpho-constitutional classification of these biominerals, providing important information on the main etiopathogenetic mechanisms. Furthermore, this approach allows a reliable selection of samples for a comprehensive mineralogical characterization essential to understand environmental implications on human health and, consequently, for biomonitoring purposes [11].

The results of the present research highlighted a lack of epidemiological studies concerning stone disease in Italy at a regional or national scale [1,3]. Although our contribution cannot provide a reliable overview of urolithiasis of the Campania region, it is doubtless an interesting focus on the mineralogical composition of uroliths extracted from patients affected by severe pathological biomineralization requiring surgical treatment.

In particular, the mineralogical frequency distribution of uroliths from the Campania region can be discussed as a function of dietary, socio-demographic, and environmental risk factors. Whewellite [$\text{CaC}_2\text{O}_4 \cdot \text{H}_2\text{O}$] and weddellite [$\text{CaC}_2\text{O}_4 \cdot (2+x)\text{H}_2\text{O}$], along with calcium oxalate anhydrous form, represent the main mineralogical phases forming the biominerals examined here. It is worth noting that the fraction of oxalates in the Campania region (ca. 51%) is quite comparable to those of other Mediterranean areas. Frequent uricite [$\text{C}_5\text{H}_4\text{N}_4\text{O}_3$] (ca. 33%), mainly observed in bladder stones of older male patients, could be related to incorrect lifestyle and dietary habits or implicating specific metabolic or genetic abnormalities.

All the issues raised from this contribution should lead to a greater awareness of the importance of knowing compositional and morphological features of pathological biominerals for the correct management of urolithiasis, adopting the mineralogical characterization of uroliths as a routine involving expertise apparently far from medical professionals. This research activity also encourages collecting data for the future development of specific tools (e.g., geographic information systems) in open access for scientists and public institutions.

Finally, one of the challenges that could affect the future of this research concerns a possible application in the engineering field. In fact, through the use of an FTIR spectral database, an attempt could be made to support an *in vivo* analysis system using optical fibers. All this could improve some surgical techniques (for example, laser lithotripsy) as the preliminary knowledge of the mineralogical composition of the urinary calculus would facilitate the operator in the instrument setting procedures.

Supplementary Materials: The following supporting information can be downloaded at: <https://www.mdpi.com/article/10.3390/min12111421/s1>, Table S1: Analytical techniques; Table S2a–d: FTIR data; Table S3: EDS data.

Author Contributions: F.I., A.L. and M.M. wrote the main manuscript text and conceptualized the research. Investigation and data visualization were carried out by F.I. in collaboration with coauthors (C.G. (Chiara Germinario), C.G. (Celestino Grifa), E.V., M.C.D.M.). A.L. and M.M. supervised the research. M.M. curated funding acquisition and project administration. L.S. and G.L. provided biominerals and clinical interviews. All authors reviewed the manuscript. All authors have read and agreed to the published version of the manuscript.

Funding: The present investigation was carried out with the financial support of the University of Sannio of Benevento (Department of Science and Technology) research funding (FRA2020 granted to Mariano Mercurio—Alessio Langella).

Data Availability Statement: All data generated or analyzed during this study are included in this published article (and its supplementary information files). The datasets used and/or analyzed during the current study are available from the corresponding author upon reasonable request.

Acknowledgments: The authors wish to thank Antonia Cinelli and Valentina Materazzo for their collaboration in the first steps of the present investigation.

Conflicts of Interest: The authors declare no conflict of interest.

References

1. Antonucci, M.; Recupero, S.M.; Marzio, V.; De Dominicis, M.; Pinto, F.; Foschi, N.; Di Gianfrancesco, L.; Bassi, P.; Ragonese, M. The impact of COVID-19 outbreak on urolithiasis emergency department admissions, hospitalizations and clinical management in central Italy: A multicentric analysis. *Actas Urol. Esp. Engl. Ed.* **2020**, *44*, 611–616. [[CrossRef](#)]
2. Croppi, E.; Ferraro, P.M.; Taddei, L.; Gambaro, G. Prevalence of renal stones in an Italian urban population: A general practice-based study. *Urol. Res.* **2012**, *40*, 517–522. [[CrossRef](#)] [[PubMed](#)]
3. Prezioso, D.; Illiano, E.; Piccinocchi, G.; Cricelli, C.; Piccinocchi, R.; Saita, A.; Micheli, C.; Trinchieri, A. Urolithiasis in Italy: An epidemiological study. *Arch. Ital. Urol. Androl.* **2014**, *86*, 99–102. [[CrossRef](#)] [[PubMed](#)]
4. Trinchieri, A.; Coppi, F.; Montanari, E.; Del Nero, A.; Zanetti, G.; Pisani, E. Increase in the prevalence of symptomatic upper urinary tract stones during the last ten years. *Eur. Urol.* **2000**, *37*, 23–25. [[CrossRef](#)]
5. Cloutier, J.; Villa, L.; Traxer, O.; Daudon, M. Kidney stone analysis: “Give me your stone, I will tell you who you are!”. *World J. Urol.* **2015**, *33*, 157–169. [[CrossRef](#)] [[PubMed](#)]
6. Daudon, M.; Dessombz, A.; Frochot, V.; Letavernier, E.; Haymann, J.P.; Jungers, P.; Bazin, D. Comprehensive morpho-constitutional analysis of urinary stones improves etiological diagnosis and therapeutic strategy of nephrolithiasis. *Comptes Rendus Chim.* **2016**, *19*, 1470–1491. [[CrossRef](#)]
7. Giannossi, M.L.; Summa, V. A Review of Pathological Biomineral Analysis Techniques and Classification Schemes. In *An Introduction to the Study of Mineralogy*; Cumhur, A., Ed.; IntechOpen: London, UK, 2012; pp. 123–146. ISBN 978-953-307-896-0.
8. Gràcia-Garcia, S.; Millán-Rodríguez, F.; Rousaud-Barón, F.; Montañés-Bermúdez, R.; Angerri-Feu, O.; Sánchez-Martín, F.; Villavicencio-Mavrich, H.; Oliver-Samper, A. Why and how we must analyze urinary calculi. *Actas Urol. Esp.* **2011**, *35*, 354–362. [[CrossRef](#)] [[PubMed](#)]
9. Daudon, M.; Bader, C.A.; Jungers, P. Urinary calculi: Review of classification methods and correlations with etiology. *Scanning Microsc.* **1993**, *7*, 1081–1086. [[PubMed](#)]
10. Daudon, M.; Jungers, P.; Bazin, D. Stone morphology: Implication for pathogenesis. In Proceedings of the AIP Conference Proceedings, Tsukuba, Japan, 12–14 March 2008; American Institute of Physics: New York, NY, USA, 2008; Volume 1049, pp. 199–215.
11. Mercurio, M.; Izzo, F.; Gatta, G.D.; Salzano, L.; Lotrecchiano, G.; Saldutto, P.; Germinario, C.; Grifa, C.; Varricchio, E.; Carafa, A. May a comprehensive mineralogical study of a jackstone calculus and some other human bladder stones unveil health and environmental implications? *Environ. Geochem. Health* **2021**, *44*, 3297–3320. [[CrossRef](#)]
12. Giannossi, M.L.; Mongelli, G.; Tateo, F.; Summa, V. Mineralogical and morphological investigation of kidney stones of a Mediterranean region (Basilicata, Italy). *J. Xray Sci. Technol.* **2012**, *20*, 175–186. [[CrossRef](#)]
13. Bazin, D.; Letavernier, E.; Haymann, J.-P.; Frochot, V.; Daudon, M. Crystalline pathologies in the human body: First steps of pathogenesis. *Ann. Biol. Clin.* **2020**, *78*, 349–362. [[CrossRef](#)] [[PubMed](#)]
14. Bazin, D.; Daudon, M.; Frochot, V.; Haymann, J.-P.; Letavernier, E. Foreword to microcrystalline pathologies: Combining clinical activity and fundamental research at the nanoscale. *Comptes Rendus Chim.* **2022**, *25*, 11–35. [[CrossRef](#)]
15. Sivaguru, M.; Saw, J.J.; Williams, J.C.; Lieske, J.C.; Krambeck, A.E.; Romero, M.F.; Chia, N.; Schwaderer, A.L.; Alcalde, R.E.; Bruce, W.J.; et al. Geobiology reveals how human kidney stones dissolve in vivo. *Sci. Rep.* **2018**, *8*, 13731. [[CrossRef](#)]
16. Abboud, I.A. Mineralogy and chemistry of urinary stones: Patients from North Jordan. *Environ. Geochem. Health* **2008**, *30*, 445–463. [[CrossRef](#)] [[PubMed](#)]
17. Afaj, A.H.; Sultan, M.A. Mineralogical composition of the urinary stones from different provinces in Iraq. *Sci. World J.* **2005**, *5*, 24–38. [[CrossRef](#)]
18. Keshavarzi, B.; Ashayeri, N.Y.; Moore, F.; Irani, D.; Asadi, S.; Zarasvandi, A.; Salari, M. Mineralogical composition of urinary stones and their frequency in patients: Relationship to gender and age. *Minerals* **2016**, *6*, 131. [[CrossRef](#)]
19. Keshavarzi, B.; Yavarashayeri, N.; Irani, D.; Moore, F.; Zarasvandi, A.; Salari, M. Trace elements in urinary stones: A preliminary investigation in Fars province, Iran. *Environ. Geochem. Health* **2015**, *37*, 377–389. [[CrossRef](#)]
20. Bazin, D.; Chevallier, P.; Matzen, G.; Jungers, P.; Daudon, M. Heavy elements in urinary stones. *Urol. Res.* **2007**, *35*, 179–184. [[CrossRef](#)]
21. Bazin, D.; Boudierlique, E.; Daudon, M.; Frochot, V.; Haymann, J.-P.; Letavernier, E.; Tielens, F.; Weil, R. Scanning electron microscopy—A powerful imaging technique for the clinician. *Comptes Rendus Chim.* **2022**, *25*, 37–60. [[CrossRef](#)]
22. Carpenter, P.; Counce, D.; Kluk, E.; Nabelek, C. Characterization of Corning EPMA Standard Glasses 95IRV, 95IRW, and 95IRX. *J. Res. Natl. Inst. Stand. Technol.* **2002**, *107*, 703–718. [[CrossRef](#)]
23. Donovan, J.J.; Hanchar, J.M.; Picolli, P.M.; Schrier, M.D.; Boatner, L.A.; Jarosewich, E. Contamination in the Rare-Earth Element Orthophosphate Reference Samples. *J. Res. Natl. Inst. Stand. Technol.* **2002**, *107*, 693–701. [[CrossRef](#)] [[PubMed](#)]
24. Donovan, J.J.; Hanchar, J.M.; Picolli, P.M.; Schrier, M.D.; Boatner, L.A.; Jarosewich, E. A re-examination of the rare-earth-element orthophosphate standards in use for electron-microprobe analysis. *Can. Mineral.* **2003**, *41*, 221–232. [[CrossRef](#)]
25. Jarosewich, E. Smithsonian Microbeam Standards. *J. Res. Natl. Inst. Stand. Technol.* **2002**, *107*, 681–685. [[CrossRef](#)] [[PubMed](#)]
26. Jarosewich, E.; White, J.S. Strontianite reference sample for electron microprobe and SEM analyses. *J. Sediment. Res.* **1987**, *57*, 762–763. [[CrossRef](#)]

27. Jarosewich, E.; Boatner, L.A. Rare-Earth Element Reference Samples for Electron Microprobe Analysis. *Geostand. Newsl.* **1991**, *15*, 397–399. [[CrossRef](#)]
28. Jarosewich, E.; MacIntyre, I.G. Carbonate reference samples for electron microprobe and scanning electron microscope analyses. *J. Sediment. Res.* **1983**, *53*, 677–678. [[CrossRef](#)]
29. Jarosewich, E.; Gooley, R.; Husler, J. Chromium Augite—A New Microprobe Reference Sample. *Geostand. Newsl.* **1987**, *11*, 197–198. [[CrossRef](#)]
30. Vicenzi, E.P.; Eggins, S.; Logan, A.; Wysoczanski, R. Microbeam Characterization of Corning Archeological Reference Glasses: New Additions to the Smithsonian Microbeam Standard Collection. *J. Res. Natl. Inst. Stand. Technol.* **2002**, *107*, 719–727. [[CrossRef](#)]
31. Pearle, M.S.; Goldfarb, D.S.; Assimos, D.G.; Curhan, G.; Denu-Ciocca, C.J.; Matlaga, B.R.; Monga, M.; Penniston, K.L.; Preminger, G.M.; Turk, T.M.T. Medical management of kidney stones: AUA guideline. *J. Urol.* **2014**, *192*, 316–324. [[CrossRef](#)]
32. Türk, C.; Donaldson, J.F.; Neisius, A.; Petrik, A.; Skolarikos, A.; Thomas, K. *EAU Guideline: Bladder Stones*; EAU Guideline Office: Arnhem, The Netherlands, 2019; ISBN 978-94-92671-07-3.
33. Türk, C.; Petrik, A.; Sarica, K.; Seitz, C.; Skolarikos, A.; Straub, M.; Knoll, T. EAU Guidelines on Interventional Treatment for Urolithiasis. *Eur. Urol.* **2016**, *69*, 475–482. [[CrossRef](#)]
34. Frassetto, L.; Kohlstadt, I. Treatment and prevention of kidney stones: An Update. *Am. Fam. Physician* **2011**, *84*, 1234–1242. [[PubMed](#)]
35. Wang, C.J.; Hsu, C.S.; Chen, H.W.; Tsai, P.C.; Chang, C.H. Long-Term Effects of Lemonade Therapy on Hypocitraturic Nephrolithiasis and Stone Recurrence: A Mini Review. *Int. J. Nephrol. Kidney Fail.* **2016**, *2*, 1–4.
36. Petit, I.; Belletti, G.D.; Debroise, T.; Llansola-Portoles, M.J.; Lucas, I.T.; Leroy, C.; Bonhomme, C.; Bonhomme-Courty, L.; Bazin, D.; Daudon, M.; et al. Vibrational Signatures of Calcium Oxalate Polyhydrates. *ChemistrySelect* **2018**, *3*, 8801–8812. [[CrossRef](#)]
37. Izatulina, A.R.; Gurzhiy, V.V.; Krzhizhanovskaya, M.G.; Kuz'mina, M.A.; Leoni, M.; Frank-Kamenetskaya, O.V. Hydrated Calcium Oxalates: Crystal Structures, Thermal Stability, and Phase Evolution. *Cryst. Growth Des.* **2018**, *18*, 5465–5478. [[CrossRef](#)]
38. Mills, S.J.; Christy, A.G. The Great Barrier Reef Expedition 1928–29: The crystal structure and occurrence of weddellite, ideally $\text{CaC}_2\text{O}_4 \cdot 2.5\text{H}_2\text{O}$, from the Low Isles, Queensland. *Mineral. Mag.* **2016**, *80*, 399–406. [[CrossRef](#)]
39. Conti, C.; Brambilla, L.; Colombo, C.; Dellasega, D.; Gatta, G.D.; Realini, M.; Zerbi, G. Stability and transformation mechanism of weddellite nanocrystals studied by X-ray diffraction and infrared spectroscopy. *Phys. Chem. Chem. Phys.* **2010**, *12*, 14560–14566. [[CrossRef](#)] [[PubMed](#)]
40. Daudon, M.; Petay, M.; Vimont, S.; Deniset, A.; Tielens, F.; Haymann, J.-P.; Letavernier, E.; Frochot, V.; Bazin, D. Urinary tract infection inducing stones: Some clinical and chemical data. *Comptes Rendus Chim.* **2022**, *25*, 315–334. [[CrossRef](#)]
41. Daudon, M.; Reveillaud, R.; Jungers, P. Piridoxilate-associated calcium oxalate urinary calculi: A new metabolic drug-induced nephrolithiasis. *Lancet* **1985**, *325*, 1338. [[CrossRef](#)]
42. Daudon, M.; Reveillaud, R.-J.; Normand, M.; Petit, C.; Jungers, P. Piridoxilate-induced calcium oxalate calculi: A new drug-induced metabolic nephrolithiasis. *J. Urol.* **1987**, *138*, 258–260. [[CrossRef](#)]
43. Abrol, N.; Kekre, N.S. Revisiting Randall's plaque. *Afr. J. Urol.* **2014**, *20*, 174–179. [[CrossRef](#)]
44. Çiftçioglu, N.; Vajdani, K.; Lee, O.; Mathew, G.; Aho, K.M.; Kajander, E.O.; McKay, D.S.; Jones, J.A.; Stoller, M.L. Association between Randall's plaque and calcifying nanoparticles. *Int. J. Nanomed.* **2008**, *3*, 105. [[CrossRef](#)] [[PubMed](#)]
45. Letavernier, E.; Bazin, D.; Daudon, M. Randall's plaque and kidney stones: Recent advances and future challenges. *Comptes Rendus Chim.* **2016**, *19*, 1456–1460. [[CrossRef](#)]
46. Cécile, V.; Dominique, B.; Léa, H.; Odile, S.; Alexandre, G.; Marie-Christine, V.; Vincent, F.; Jean-Philippe, H.; Isabelle, B.; Olivier, T.; et al. Topography, Composition and Structure of Incipient Randall Plaque at the Nanoscale Level. *J. Urol.* **2016**, *196*, 1566–1574. [[CrossRef](#)]
47. Gay, C.; Letavernier, E.; Verpont, M.-C.; Walls, M.; Bazin, D.; Daudon, M.; Nassif, N.; Stéphan, O.; de Frutos, M. Nanoscale Analysis of Randall's Plaques by Electron Energy Loss Spectromicroscopy: Insight in Early Biomineral Formation in Human Kidney. *ACS Nano* **2020**, *14*, 1823–1836. [[CrossRef](#)] [[PubMed](#)]
48. Bazin, D.; Leroy, C.; Tielens, F.; Bonhomme, C.; Bonhomme-Courty, L.; Damay, F.; Le Denmat, D.; Sadoine, J.; Rode, J.; Frochot, V. Hyperoxaluria is related to whewellite and hypercalciuria to weddellite: What happens when crystalline conversion occurs? *Comptes Rendus Chim.* **2016**, *19*, 1492–1503. [[CrossRef](#)]
49. Gibson, R.I. Descriptive human pathological mineralogy. *Am. Mineral. J. Earth Planet. Mater.* **1974**, *59*, 1177–1182.
50. Zhao, W.; Sharma, N.; Jones, F.; Raiteri, P.; Gale, J.D.; Demichelis, R. Anhydrous calcium oxalate polymorphism: A combined computational and synchrotron X-ray diffraction study. *Cryst. Growth Des.* **2016**, *16*, 5954–5965. [[CrossRef](#)]
51. Hocart, R.; Watelle-Marion, G.; Thrierr-Sorel, G.; Gerard, A. Nature topotactique de la deshydratation. *Acad. Sci. Paris* **1965**, *261*, 2363–2366.
52. Oztoprak, B.G.; Gonzalez, J.; Yoo, J.; Gulecen, T.; Mutlu, N.; Russo, R.E.; Gundogdu, O.; Demir, A. Analysis and classification of heterogeneous kidney stones using laser-induced breakdown spectroscopy (LIBS). *Appl. Spectrosc.* **2012**, *66*, 1353–1361. [[CrossRef](#)]
53. Srivastava, A.; Swain, K.; Ajith, N.; Wagh, D.; Acharya, R.; Reddy, A.; Mete, U. Trace element study of kidney stones from subjects belonging to stone belt region of India. *J. Radioanal. Nucl. Chem.* **2012**, *294*, 425–428. [[CrossRef](#)]
54. Primiano, A.; Persichilli, S.; Gambaro, G.; Ferraro, P.M.; D'Addessi, A.; Cocci, A.; Schiattarella, A.; Zuppi, C.; Gervasoni, J. FT-IR analysis of urinary stones: A helpful tool for clinician comparison with the chemical spot test. *Dis. Markers* **2014**, *2014*, 176165. [[CrossRef](#)]

55. Aslin Shamema, A.; Thanigai Arul, K.; Senthil Kumar, R.; Kalkura, S.N. Physicochemical analysis of urinary stones from Dharmapuri district. *Spectrochim. Acta—Part A Mol. Biomol. Spectrosc.* **2015**, *134*, 442–448. [[CrossRef](#)] [[PubMed](#)]
56. Sekkoum, K.; Cheriti, A.; Taleb, S.; Belboukhari, N. FTIR spectroscopic study of human urinary stones from El Bayadh district (Algeria). *Arab. J. Chem.* **2016**, *9*, 330–334. [[CrossRef](#)]
57. Pinto, B.; Rocha, E.; Ruiz-Marcellán, F.J. Isolation and characterization of uric acid stones. *Kidney Int.* **1976**, *10*, 437–443. [[CrossRef](#)] [[PubMed](#)]
58. Evan, A.P.; Lingeman, J.E.; Coe, F.L.; Shao, Y.; Parks, J.H.; Bledsoe, S.B.; Phillips, C.L.; Bonsib, S.; Worcester, E.M.; Sommer, A.J.; et al. Crystal-associated nephropathy in patients with brushite nephrolithiasis. *Kidney Int.* **2005**, *67*, 576–591. [[CrossRef](#)] [[PubMed](#)]
59. Klee, L.W.; Brito, C.G.; Lingeman, J.E. The clinical implications of brushite calculi. *J. Urol.* **1991**, *145*, 715–718. [[CrossRef](#)]
60. Berzina-Cimdina, L.; Borodajenko, N. Research of Calcium Phosphates Using Fourier Transform Infrared Spectroscopy. In *Infrared Spectroscopy—Materials Science, Engineering and Technology*; IntechOpen: London, UK, 2012; pp. 123–148.
61. Medina, E.; Romero, C.; García, P.; Brenes, M. Characterization of bioactive compounds in commercial olive leaf extracts, and olive leaves and their infusions. *Food Funct.* **2019**, *10*, 4716–4724. [[CrossRef](#)]
62. Chatterjee, P.; Chakraborty, A.; Mukherjee, A.K. Phase composition and morphological characterization of human kidney stones using IR spectroscopy, scanning electron microscopy and X-ray Rietveld analysis. *Spectrochim. Acta—Part A Mol. Biomol. Spectrosc.* **2018**, *200*, 33–42. [[CrossRef](#)]
63. Kanchana, G.; Sundaramoorthi, P.; Jeyanthi, G.P. Bio-Chemical Analysis and FTIR-Spectral Studies of Artificially Removed Renal Stone Mineral Constituents. *J. Miner. Mater. Charact. Eng.* **2009**, *8*, 161–170. [[CrossRef](#)]
64. Selvaraju, R.; Raja, A.; Thirupathi, G. FT-IR spectroscopic, thermal analysis of human urinary stones and their characterization. *Spectrochim. Acta—Part A Mol. Biomol. Spectrosc.* **2015**, *137*, 1397–1402. [[CrossRef](#)]
65. Wilson, E.V.; Bushiri, M.J.; Vaidyan, V.K. Characterization and FTIR spectral studies of human urinary stones from Southern India. *Spectrochim. Acta—Part A Mol. Biomol. Spectrosc.* **2010**, *77*, 442–445. [[CrossRef](#)] [[PubMed](#)]
66. Carpentier, X.; Daudon, M.; Traxer, O.; Jungers, P.; Mazouyes, A.; Matzen, G.; Véron, E.; Bazin, D. Relationships between carbonation rate of carbapatite and morphologic characteristics of calcium phosphate stones and etiology. *Urology* **2009**, *73*, 968–975. [[CrossRef](#)] [[PubMed](#)]
67. Griffith, D.P. Infection-induced renal calculi. *Kidney Int.* **1982**, *21*, 422–430. [[CrossRef](#)] [[PubMed](#)]
68. Kono, T.; Sakae, T.; Nakada, H.; Kaneda, T.; Okada, H. Confusion between Carbonate Apatite and Biological Apatite (Carbonated Hydroxyapatite) in Bone and Teeth. *Minerals* **2022**, *12*, 170. [[CrossRef](#)]
69. Coe, F.L.; Coe, F. Uric acid and calcium oxalate nephrolithiasis. *Kidney Int.* **1983**, *24*, 392–403. [[CrossRef](#)]
70. Bouzidi, H.; de Brauwere, D.; Daudon, M. Does urinary stone composition and morphology help for prediction of primary hyperparathyroidism? *Nephrol. Dial. Transplant.* **2011**, *26*, 565–572. [[CrossRef](#)]
71. Daudon, M.; Bouzidi, H.; Bazin, D. Composition and morphology of phosphate stones and their relation with etiology. *Urol. Res.* **2010**, *38*, 459–467. [[CrossRef](#)]
72. Gault, M.H.; Chafe, L.L.; Morgan, J.M.; Parfrey, P.S.; Harnett, J.D.; Walsh, E.A.; Prabhakaran, V.M.; Dow, D.; Colpitts, A. Comparison of patients with idiopathic calcium phosphate and calcium oxalate stones. *Medicine* **1991**, *70*, 345–359. [[CrossRef](#)]
73. Konnak, J.W.; Kogan, B.A.; Lau, K. Renal calculi associated with incomplete distal renal tubular acidosis. *J. Urol.* **1982**, *128*, 900–902. [[CrossRef](#)]
74. Pak, C.Y.C.; Poindexter, J.R.; Adams-Huet, B.; Pearle, M.S. Predictive value of kidney stone composition in the detection of metabolic abnormalities. *Am. J. Med.* **2003**, *115*, 26–32. [[CrossRef](#)]
75. Sorokin, I.; Mamoulakis, C.; Miyazawa, K.; Rodgers, A.; Talati, J.; Lotan, Y. Epidemiology of stone disease across the world. *World J. Urol.* **2017**, *35*, 1301–1320. [[CrossRef](#)] [[PubMed](#)]
76. Curhan, G.C. Epidemiology of stone disease. *Urol. Clin. N. Am.* **2007**, *34*, 287–293. [[CrossRef](#)] [[PubMed](#)]
77. Liu, Y.; Chen, Y.; Liao, B.; Luo, D.; Wang, K.; Li, H.; Zeng, G. Epidemiology of urolithiasis in Asia. *Asian J. Urol.* **2018**, *5*, 205–214. [[CrossRef](#)] [[PubMed](#)]
78. Hornberger, B.; Bollner, M.R. Kidney stones. *Physician Assist. Clin.* **2018**, *3*, 37–54. [[CrossRef](#)]
79. Scales, C.D., Jr.; Smith, A.C.; Hanley, J.M.; Saigal, C.S.; Urologic Diseases in America Project. Prevalence of kidney stones in the United States. *Eur. Urol.* **2012**, *62*, 160–165. [[CrossRef](#)] [[PubMed](#)]
80. Pugliese, J.M.; Baker, K.C. Epidemiology of nephrolithiasis in personnel returning from Operation Iraqi Freedom. *Urology* **2009**, *74*, 56–60. [[CrossRef](#)] [[PubMed](#)]
81. Ahmad, F.; Nada, M.O.; Bin Farid, A.; Haleem, M.A.; Razack, S.M.A. Epidemiology of urolithiasis with emphasis on ultrasound detection: A retrospective analysis of 5371 cases in Saudi Arabia. *Saudi J. Kidney Dis. Transplant.* **2015**, *26*, 386. [[CrossRef](#)] [[PubMed](#)]
82. AURO. *Linea Guida per la Calcolosi Delle vie Urinarie*; Associazione Urologi Italiani: Pietra Ligure, Italy, 2007.
83. Daudon, M.; Doré, J.-C.; Jungers, P.; Lacour, B. Changes in stone composition according to age and gender of patients: A multivariate epidemiological approach. *Urol. Res.* **2004**, *32*, 241–247. [[CrossRef](#)]
84. Yasui, T.; Iguchi, M.; Suzuki, S.; Okada, A.; Itoh, Y.; Tozawa, K.; Kohri, K. Prevalence and epidemiologic characteristics of lower urinary tract stones in Japan. *Urology* **2008**, *72*, 1001–1005. [[CrossRef](#)]
85. Yasui, T.; Iguchi, M.; Suzuki, S.; Kohri, K. Prevalence and epidemiological characteristics of urolithiasis in Japan: National trends between 1965 and 2005. *Urology* **2008**, *71*, 209–213. [[CrossRef](#)]

86. Grases, F.; Costa-Bauzá, A.; Ramis, M.; Montesinos, V.; Conte, A. Simple classification of renal calculi closely related to their micromorphology and etiology. *Clin. Chim. Acta* **2002**, *322*, 29–36. [[CrossRef](#)]
87. Shokouhi, B.; Gasemi, K.; Norizadeh, E. Chemical composition and epidemiological risk factors of urolithiasis in Ardabil Iran. *Res. J. Biol. Sci.* **2008**, *3*, 620–626.
88. Wu, W.; Yang, D.; Tiselius, H.-G.; Ou, L.; Liang, Y.; Zhu, H.; Li, S.; Zeng, G. The characteristics of the stone and urine composition in Chinese stone formers: Primary report of a single-center results. *Urology* **2014**, *83*, 732–737. [[CrossRef](#)] [[PubMed](#)]
89. Wu, W.; Yang, B.; Ou, L.; Liang, Y.; Wan, S.; Li, S.; Zeng, G. Urinary stone analysis on 12,846 patients: A report from a single center in China. *Urolithiasis* **2014**, *42*, 39–43. [[CrossRef](#)] [[PubMed](#)]
90. Diangienda, P.K.D.; Moningo, D.M.; Makulo, J.-R.R.; Sumaili, E.K.; Mafuta, E.M.; Mayindu, A.N.; Punga-Maole, A.M.L.; Haymann, J.-P.; Daudon, M. Morpho-constitutional analysis of urinary stones from patients with urolithiasis in the Democratic Republic of Congo. *Afr. J. Urol.* **2021**, *27*, 99. [[CrossRef](#)]
91. Diangienda, P.K.D.; Moningo, D.M.; Mayindu, A.N.; Haymann, J.-P.; Daudon, M. Heavy metals in urinary stones in the Democratic Republic of Congo. *Afr. J. Urol.* **2021**, *27*, 1–9. [[CrossRef](#)]
92. Diasiama, P.D.K.; Molamba, D.M.; Rissasy, J.-R.M.; Kiswaya, E.S.; Musalu, É.M.; Ngoma, A.; Nkumu, M.L.; Punga-Maole, A.; Nkandi, S.L.L.; Haymann, J.-P. Composition chimique des calculs urinaires et caractéristiques épidémiologiques associées en République Démocratique du Congo. *Néphrol. Théor.* **2021**, *17*, 441–450. [[CrossRef](#)]
93. Mbonu, O.; Attah, C.H.; Ikeakor, I. Urolithiasis in an African population. *Int. Urol. Nephrol.* **1984**, *16*, 291–296. [[CrossRef](#)]
94. Moser, R.; Zaccarini, F.; Alber, T.; Kerbl, R. First finding of tiemannite, HgSe, in human bladder stones: An electron microprobe study. *Micron* **2020**, *138*, 102928. [[CrossRef](#)]
95. Romero, V.; Akpınar, H.; Assimos, D.G. Kidney stones: A global picture of prevalence, incidence, and associated risk factors. *Rev. Urol.* **2010**, *12*, e86. [[CrossRef](#)]
96. Novikov, A.; Nazarov, T.; Startsev, V.Y. Epidemiology of stone disease in the Russian Federation and Post-Soviet era. In *Urolithiasis*; Springer: London, UK, 2012; pp. 97–105.
97. Bae, S.R.; Seong, J.-M.; Kim, L.Y.; Paick, S.H.; Kim, H.G.; Lho, Y.S.; Park, H.K. The epidemiology of reno-ureteral stone disease in Koreans: A nationwide population-based study. *Urolithiasis* **2014**, *42*, 109–114. [[CrossRef](#)] [[PubMed](#)]
98. Brikowski, T.H.; Lotan, Y.; Pearle, M.S. Climate-related increase in the prevalence of urolithiasis in the United States. *Proc. Natl. Acad. Sci. USA* **2008**, *105*, 9841–9846. [[CrossRef](#)] [[PubMed](#)]
99. Izzo, F.; Furno, A.; Cilenti, F.; Germinario, C.; Gorrasi, M.; Mercurio, M.; Langella, A.; Grifa, C. The domus domini imperatoris Apicii built by Frederick II along the Ancient Via Appia (southern Italy): An example of damage diagnosis for a Medieval monument in rural environment. *Constr. Build. Mater.* **2020**, *259*, 119718. [[CrossRef](#)]
100. Kuta, J.; Machát, J.; Benová, D.; Červenka, R.; Kořistková, T. Urinary calculi—Atypical source of information on mercury in human biomonitoring. *Cent. Eur. J. Chem.* **2012**, *10*, 1475–1483. [[CrossRef](#)]
101. Kuta, J.; Machát, J.; Benová, D.; Červenka, R.; Zeman, J.; Martinec, P. Association of minor and trace elements with mineralogical constituents of urinary stones: A hard nut to crack in existing studies of urolithiasis. *Environ. Geochem. Health* **2013**, *35*, 511–522. [[CrossRef](#)]
102. Singh, V.K.; Rai, P.K. Kidney stone analysis techniques and the role of major and trace elements on their pathogenesis: A review. *Biophys. Rev.* **2014**, *6*, 291–310. [[CrossRef](#)]
103. Giannossi, M.L.; Summa, V.; Mongelli, G. Trace element investigations in urinary stones: A preliminary pilot case in Basilicata (Southern Italy). *J. Trace Elem. Med. Biol.* **2013**, *27*, 91–97. [[CrossRef](#)]
104. Madore, F.; Stampfer, M.J.; Rimm, E.B.; Curhan, G.C. Nephrolithiasis and risk of hypertension. *Am. J. Hypertens.* **1998**, *11*, 46–53. [[CrossRef](#)]
105. Reiner, A.P.; Kahn, A.; Eisner, B.H.; Pletcher, M.J.; Sadetsky, N.; Williams, O.D.; Polak, J.F.; Jacobs, D.R.; Stoller, M.L. Kidney stones and subclinical atherosclerosis in young adults: The CARDIA study. *J. Urol.* **2011**, *185*, 920–925. [[CrossRef](#)]
106. Luo, W.; Zhou, Y.; Gao, C.; Yan, P.; Xu, L. Urolithiasis, Independent of Uric Acid, Increased Risk of Coronary Artery and Carotid Atherosclerosis: A Meta-Analysis of Observational Studies. *Biomed Res. Int.* **2020**, *2020*, 1026240. [[CrossRef](#)]
107. Bao, Y.; Wei, Q. Water for preventing urinary stones. *Cochrane Database Syst. Rev.* **2012**, *2*, CD004292. [[CrossRef](#)] [[PubMed](#)]
108. Taylor, E.N.; Fung, T.T.; Curhan, G.C. DASH-style diet associates with reduced risk for kidney stones. *J. Am. Soc. Nephrol.* **2009**, *20*, 2253–2259. [[CrossRef](#)] [[PubMed](#)]
109. De Vita, P.; Allocca, V.; Celico, F.; Fabbrocino, S.; Mattia, C.; Monacelli, G.; Musilli, I.; Piscopo, V.; Scalise, A.R.; Summa, G. Hydrogeology of continental southern Italy. *J. Maps* **2018**, *14*, 230–241. [[CrossRef](#)]
110. Borghi, L.; Meschi, T.; Amato, F.; Briganti, A.; Novarini, A.; Giannini, A. Urinary volume, water and recurrences in idiopathic calcium nephrolithiasis: A 5-year randomized prospective study. *J. Urol.* **1996**, *155*, 839–843. [[CrossRef](#)]